IR study on the electrochemical reduction of nimesulide

S. Stoyanov[*], D. Yancheva, A. Kosateva

Department of Structural Organic Analysis, Institute of Organic Chemistry with Centre of Phytochemistry, Bulgarian Academy of Sciences, Acad. G. Bonchev Str., build. 9, 1113 Sofia, Bulgaria

Dedicated to Acad. Ivan Juchnovski on the occasion of his 80th birthday

The electrochemical reduction of the nonsteroidal anti-inflammatory drug nimesulide, N-(4-nitro-2-phenoxyphenyl)-methanesulfone anilide, was performed in DMSO-d_6 solution and the IR spectral changes arising from the conversion were monitored. The spectral studies showed that in these conditions, electrochemical reduction leads to considerable decrease of the N-O and S-O stretching frequencies, increase of the C-NO_2 stretching frequency and disappearance of δ(N-H). Based on comparison with theoretically predicted spectra of possible reduction products, the observed changes were attributed to the generation of dianion radical of nimesulide. The IR frequency shifts indicated that essential structural changes in the nitro, sulfonamide group and the phenyl ring connecting them have occurred as a result of the reduction. NBO charge and spin density calculations showed that 71% of the spin density is localized into the nitro group of the dianion radical, whereas 87% of the anionic charge is concentrated into the sulfonamide fragment.

Key words: nimesulide; nitro reduction; electrochemical reduction; IR spectroscopy; dianion radical

INTRODUCTION

N-(4-nitro-2-phenoxyphenyl)-methanesulfone anilide (**1**) is a nonsteroidal anti-inflammatory drug (NSAID) that has potent analgesic, anti-inflammatory and antipyretic activities on oral and rectal administration [1]. It is a preferential cyclo-oxygenase-2 (COX-2) inhibitor hence inhibits the synthesis of destructive prostaglandins and spares cytoprotective prostaglandins [2]. In addition, some studies had mainly attributed the selective inhibition of COX-2 and the anti-inflammatory effect of nimesulide to its radical scavenger behaviour, which may be explained by the presence of a methanesulfonamide group that has strong interactions with the COX-2 enzyme [1,3].

Nimesulide as other nitroaromatic drugs, has been associated with rare and unpredictable but serious hepatic adverse reactions [4,5]. What the nitroaromatic drugs have in common is their potential to undergo multistep nitroreductive bioactivation (6-electron transfer) that produces the potentially hazardous nitroanion radical, nitroso intermediate, and N-hydroxy derivative. These intermediates have been associated with increased oxidant stress and targeting of nucleophilic residues on proteins and nucleic acids [5]. It was shown that in humans nimesulide is oxidatively metabolized to 4'-hydroxynimesulide but also nitroreduced to the amine (with subsequent conjugation) [6,7].

However, the role of the reactive intermediates, resulting from the transformation could not be clarified, presumably due to their short life-time and inability to detect them by conventional analysis of metabolites [8]. In addition, it is not known which nitroreductase(s) play a role in these reactions. In rats, nimesulide was reduced to its amino metabolite, similar to humans [9]. Interestingly, anaerobic incubation increased the nitroreductive pathway, while the formation of 4'-hydroxylated nimesulide (CYP-mediated and therefore oxygen-dependent) was completely blocked. Under anaerobic conditions, the nitroreductive pathway is enhanced, while the formation of 4'-hydroxylated nimesulide, which is mediated by CYP in presence of oxygen, is blocked [5,9]. Given the complexity of the multiple competing reactions, it was suggested that the imbalance between the oxidative and reducing pathways of nimesulide and the relative abundance of molecular oxygen might be the crucial starting events in the pro-toxic processes in the liver [5].

The redox behaviour of nimesulide was previously studied by cyclic voltametry in efforts to understand its metabolism and mechanism of hepatotoxicity [10-12]. These electrochemical measurements showed that the reduction of nimesulide is strongly dependent on the nature of the media, following different reduction behavior. It was demonstrated that a stable free radical product was successfully electrogenerated in mixed

---

media, containing DMF(60%) and citrate buffer (40%), while in protic mixture of Britton Rhobinson buffer (70%) and KCl-ethanol solution (30%) a radical species could be observed only in strong alkaline media (pH 12) [12]. In protic medium at pH 9, nimesulide was converted directly to hydroxylamine [12].

Monitoring of the IR spectral changes in the course of electrochemical reduction of nimesulide offers a convenient way to complement the information gathered by the cyclovoltametric studies. Earlier studies has proven that the structural changes arising from the conversion of various organic carbonyl, nitrile and nitro compounds can be reliably described based on the observed shifts of their characteristic IR absorptions, especially when supported by theoretical computations [13-23]. Herein we present our study on the IR spectral and structural changes related to the electrochemical reduction of nimesulide.

EXPERIMENTAL AND COMPUTATIONS

Nimesulide (99%), tetrabutylammonium bromide (99%) and spectral quality DMSO-d_6 were purchased from Sigma-Aldrich Co. All spectra were measured on a Bruker Tensor 27 FT spectrometer by accumulating 64 scans at 2 cm^{-1} resolution. The electrochemical transformation of nimesulide was performed in a special CaF$_2$ cell with platinum electrodes, filled with 0.1 M solution of nimesulide in DMSO-d_6 and equavimolar amount of tetrabutylammonium bromide. 4.5 V voltage was applied, and the spectra were measured in 10 minutes interval. The measurements were carried out for 75 min to gain maximum conversion. After that the polarity of electrodes was reversed and the measurements continued for the same interval.

All quantum chemistry calculations were performed using Gaussian 09 package of programs [24]. Geometry and vibrational frequencies of the species studied were performed by an analytical gradient technique without any symmetry constraint. All the results were obtained using the density functional theory (DFT), employing the B3LYP (Becke's three-parameter non-local exchange correlation) functional [25], 6-311++G** and 6-311++G(2df,2dp) basis sets. Incorporation of DMSO solvent was performed by the Integral Equation Formalism of Polarizable Continuum Model (IEFPCM) [26,27]. The stationary points found on the potential energy hypersurfaces for

each structure were characterized using the standard harmonic vibrational analysis. A standard least-squares program has been used to calculate single parameter regression indices. The absence of imaginary frequencies confirmed that the stationary points corresponded to local minima on the potential hypersurfaces.

RESULTS AND DISCUSSION

The IR spectral measurements during electrochemical reduction are typically performed in DMSO-d_6 solution with tetrabutylammonium bromide as electrolyte salt [13-23]. In these conditions it is expected that the radical anion product will be generated and stabilized in measurable amounts. In order to achieve an accurate and reliable description of the changes resulting from the electrochemical reduction of nimesulide, several initial studies were done prior the IR measurements:
(i) Optimization of the molecular structure of nimesulide and possible reduction products,
(ii) Assignment of the characteristic IR bands of nimesulide in DMSO-d_6 solution,
(iii) Prediction of the IR spectra of possible reduction products.

Having in mind the strong dependence of the reduction behavior on the nature of the media, we took into account a radical anion resulting from one-electron reduction (**2**) and a dianion radical resulting from one-electron reduction accompanied by deprotonation (**3**) in the analysis of possible reduction products.

Optimization of the molecular structure of nimesulide and possible reduction products

X-ray studies have reported three polymorphic forms of nimesulide, which are distinguished by different steric positions of the sulfonamide fragment and ring B [28-31]. Our computations showed that nimesulide has two stable conformations in DMSO solution differing by the torsion angle of the sulfomethyl group (Figure 1). In both forms the nitro and amino group lie in the plane of benzene ring A. Ring B lies in another plane with dihedral angle 77° towards ring A. The structure is stabilized by formation of an intramolecular hydrogen bond between the sulfonamide N-H and the phenoxy O-atom. The sulfomethyl group might be above (**1a**) or below (**1b**) the plane of benzene ring A. The two forms give indiscernible IR spectra.
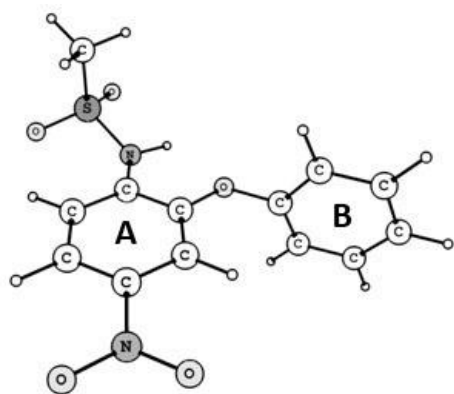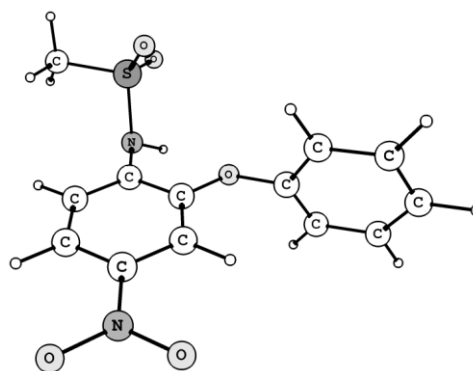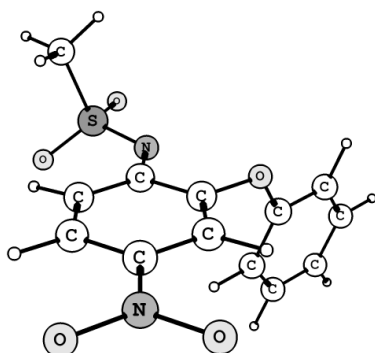
Nimesulide molecule **1a**
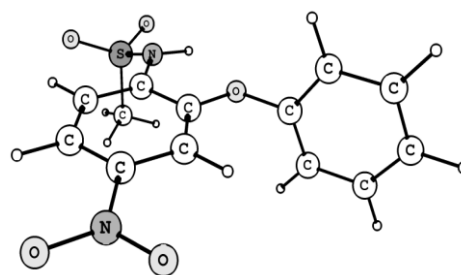
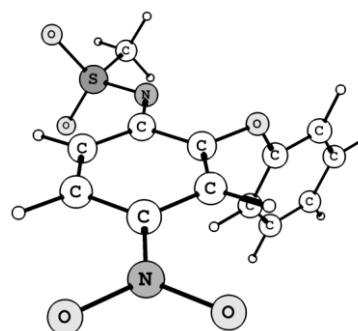Nimesulide molecule **1b** ($\Delta E = + 0.003$ kJ.mol^{-1})
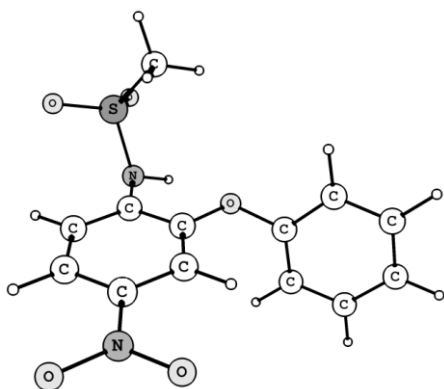
Radical anion **2a**
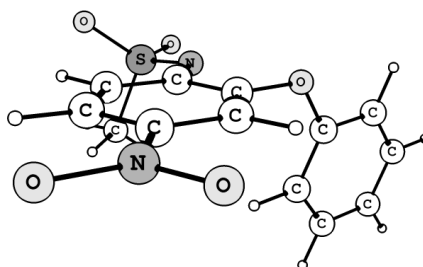
Radical anion **2b** ($\Delta E = + 4.97$ kJ.mol^{-1})

Dianion radical **3a**

Dianion radical **3b** ($\Delta E = + 0.21$ kJ.mol^{-1})

Dianion radical **3c** ($\Delta E = + 0.32$ kJ.mol^{-1})

Fig. 1. Different possible conformers of nimesulide molecule **1**, its radical-anion **2**, and dianion-radical **3**, computed at 6-311++G** theory level.

The conformational flexibility of the radical species is also considerable as can be seen by the small energy differences between their conformers. Two stable conformations of radical anion **2** were found (Figure 1) resembling closely those of the neutral nimesulide. The theoretical data for dianion radical **3** showed the presence of at least three conformers, which are characterized by very low energy differences (Figure 1).

Assignment of the characteristic IR bands of nimesulide in DMSO-d_6 solution

The strongest and most characteristic bands of nimesulide were observed in the 1700-1100 cm^{-1} region (Figure 2). The bands at 1523 and 1340 cm^{-1} (Table 1) can be assigned to the nitro asymmetrical and symmetrical vibration.

Table 1. Theoretical and experimental frequencies and intensities for nimesulide molecule **1**.

No	Theoretical data (B3LYP/6-311++G(2df,2dp))			Experimental data (DMSO-d$_6$[a])	
	$\nu_{theor.}$[b]	A[c]	Approximate description[d]	$\nu_{exp.}$	A[e]
1.	3396	197	ν(N-H)	_[f]	_[f]
2.	3098	12	ν_{PhA}(C-H)	_[g]	_[g]
3.	3097	4	ν_{PhA}(C-H)	_[g]	_[g]
4.	3086	2	ν_{PhA}(C-H)	_[g]	_[g]
5.	3063	4	ν_{PhB}(C-H)	_[g]	_[g]
6.	3058	12	ν_{PhB}(C-H)	_[g]	_[g]
7.	3053	23	ν_{PhB}(C-H)	_[g]	_[g]
8.	3045	8	ν_{PhB}(C-H)	_[g]	_[g]
9.	3038	0	ν^{as}(CH$_3$)	_[g]	_[g]
10.	3037	0	ν_{PhA}(C-H), ν_{PhB}(C-H)	_[g]	_[g]
11.	3026	1	ν^{as}(CH$_3$)	_[g]	_[g]
12.	2937	0	ν^{s}(CH$_3$)	_[g]	_[g]
13.	1607	4	ν_{PhA}(C=C), ν_{PhB}(C=C)	_[g]	_[g]
14.	1601	11	ν_{PhB}(C=C)	_[g]	_[g]
15.	1598	67	ν_{PhA}(C=C), ν_{PhB}(C=C)	1597	m
16.	1593	194	ν_{PhA}(C=C), ν_{PhB}(C=C)	1587	m
17.	1507	550	ν^{as}(NO$_2$), δ(N-H)	1523	s
18.	1500	88	δ_{PhB}(C-H)	1501	sh
19.	1499	431	δ_{PhB}(CH), ν^{as}(NO$_2$)	1490	s
20.	1467	3	δ_{PhB}(CH)	_[g]	_[g]
21.	1443	107	δ(NH)	1457	w, br
22.	1433	5	δ^{as}(CH$_3$)	_[g]	_[g]
23.	1432	9	δ^{as}(CH$_3$)	_[g]	_[g]
24.	1413	214	δ(N-H), ν_{PhA}(C=C)	1411	w, br
25.	1356	69	ν_{PhA}(C=C), ν(C-N)	_[g]	_[g]
26.	1345	14	δ^{s}(CH$_3$)	_[g]	_[g]
27.	1337	0	δ_{PhB}(CH)	_[g]	_[g]
28.	1329	901	ν^{s}(NO$_2$), δ^{PhB}(CH)	1340	vs
29.	1312	10	δ_{PhB}(CH)	_[g]	_[g]
30.	1308	466	ν^{as}(SO$_2$), δ_{PhB}(CH)	1291	w
31.	1291	387	ν(C-NH), δ_{PhB}(CH)	1281	w
32.	1257	736	ν(C-OC), δ_{PhA}(CH)	1250	m
33.	1227	344	ν(C-OC), δ_{PhB}(CH)	1217	m
34.	1199	52	δ_{PhA}(CH), δ(C-OC)	_[g]	_[g]
35.	1182	34	δ_{PhA}(CH), δ(C-OC)	_[g]	_[g]
36.	1181	2	δ_{PhB}(CH)	_[g]	_[g]
37.	1157	41	δ_{PhA}(CH)	_[g]	_[g]
38.[h]	1139	471	ν^{s}(SO$_2$)	1159	s
MAD[i]	-	-	-	*9.5*	-

[a] Measured after having decomposed the complex bands into components; [b] Infrared frequencies [cm^{-1}] scaled by Eqn. (1).[c] Predicted intensities [km.mol^{-1}]; [d] Vibrational modes: ν, stretching; δ, in-plane bending; γ, out-of-plane bending; superscripts: s, symmetrical; as – asymmetrical; PhA, phenyl ring A; PhB - phenyl ring B; [e] Relative intensities: vw, very weak; w, weak; m, moderate; s, strong; vs, very strong; sh, shoulder; br, broad; [f] This frequency was removed from correlation analysis, because there is significant association between the amide group and the solvent molecules; [g] These bands were not detected in the IR spectrum; [h] Followed by 28 lower-frequency vibrations that could not be observed experimentally due to self-absorptions of DMSO-d$_6$ below 1100 cm^{-1}; [i] Mean Absolute Deviation between theoretically predicted and experimentally observed vibrational frequencies.

Two weaker bands observed at 1291 and 1159 cm^{-1} could be attributed to the asymmetrical and symmetrical stretching of the SO_2 group. The NH deformation is characterized by a weak broad band with maximum at 1411 cm^{-1}. The bands for C-N and S-N stretching are expected below 1100 cm^{-1} and could not be observed due to self-absorptions of DMSO-d$_6$.

The experimental IR frequencies were accurately reproduced by the IEF-PCM B3LYP/6-311++G(2df,2dp) calculations. After comparison of the theoretical frequencies to the experimental values the following scaling equation was obtained:

$$\nu^{scaled} = 0.92992 + 84.2 \left(cm^{-1} \right)$$

It was applied in the following IR analysis to scale the native theoretical frequencies of the radical species **2** and **3** calculated at same theory level.
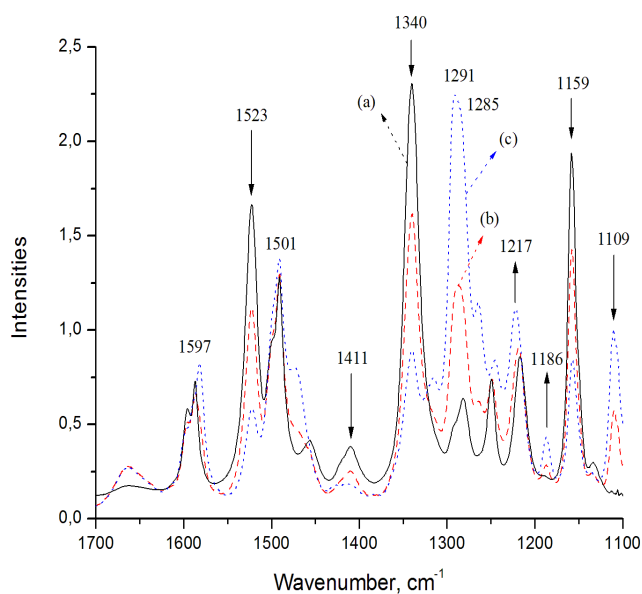

Fig. 2. IR spectra of nimesulide before reduction, t = 0 min (a) and in the course of electrochemical reduction, t = 30 min (b), t = 75 min (c).

IR measurements in the course of electrochemical reduction of nimesulide

In the course of electrochemical reduction of nimesulide, the intensities of the bands at 1523 and 1340 cm^{-1} decreased (Figure 2). The same was observed also for the band of the SO_2 symmetrical stretching at 1159 cm^{-1}. The band for NH deformation at 1411 cm^{-1} nearly disappeared. In the

same time, new bands appeared at 1291, 1217, 1186 and 1109 cm^{-1}. Two new bands – at 1225 and 1347 cm^{-1}, were detected like shoulders.

The intensities of the newly appeared bands gradually increased over time. Reversal in the polarity of the electrolysis cell restored the original spectrum of **1** which led to the conclusion that the observed spectral changes are due to reduction of nimesulide and not to products of radical recombination or other chemical transformations.

Interpretation of the IR data

Due to the broadening and overlapping of the bands, the assignment of the exact positions of experimental bands was done by second derivative analysis and curve fitting procedure. The frequencies of all bands appearing in the course of electrochemical reduction of nimesulide were thoroughly compared with the theoretically calculated frequencies of possible products – radical anion **2** and radical dianion **3**.

According to the theoretically calculated frequencies of **2** and **3,** in both cases of $\nu^{as}(NO_2)$ and $\nu^s(NO_2)$ should strongly decrease, while $\nu(C-NO_2)$ should considerably increase. The positions of the phenyl bands are not expected to change strongly. However, the magnitude of the nitro frequencies shift and the spectral changes concerning the other functional groups allow discrimination between the two products.

Upon conversion in **2**, the band for $\nu^{as}(NO_2)$ is expected to appear at 1257 cm^{-1} ($\Delta\nu = - 273$ cm[-1]); $\nu^s(NO_2)$ – at 1055 cm^{-1} ($\Delta\nu = - 274$ cm[-1]); and $\nu(C-NO_2)$ – at 1365 cm^{-1} ($\Delta\nu = + 265$ cm[-1]) (Table S1). These changes are similar to those, observed earlier for other nitrophenyl derivatives [13-16,22,23]. The band for $\delta(N-H)$ is expected to shift only slightly. $\nu^{as}(SO_2)$ and $\nu^s(SO_2)$ should be lowered weakly, only by 19 and 2 cm^{-1}.

Conversion in **3** should lead to the following changes: the band for $\nu^{as}(NO_2)$ would shift to 1227 cm^{-1} ($\Delta\nu = - 303$ cm[-1]); $\nu^s(NO_2)$ – to 1057 cm^{-1} ($\Delta\nu = - 283$ cm[-1]); and $\nu(C-NO_2)$ – to 1348 cm^{-1} ($\Delta\nu = + 248$ cm[-1]) (Table 2). The band for $\delta(N-H)$ should disappear as a result of deprotonation, while $\nu^{as}(SO_2)$ and $\nu^s(SO_2)$ should be lowered significantly by 105 and 75 cm^{-1}. $\nu(C-NSO_2)$ should produce a very strong band at 1298 cm^{-1}.

Based on these assignments, better matching was found with the spectrum of radical dianion **3**

(Table 2). The experimental bands at 1347 and 1225 cm^{-1} were attributed to ν(C-NO$_2$) and ν^{as}(NO$_2$) of radical dianion **3**. Deprotonation was evidenced by the nearly complete disappearance of the band for δ(N-H). Another prove for the conversion of **1** in **3** was found in the appearance of the strong doublet with maximum around 1290 cm^{-1} (1294

and 1285 cm^{-1} after deconvolution) which agrees well with the predicted positions and strong intensities of ν(C-NSO$_2$) and ν_{PhA}(C=C) - number 26 and 27 in Table 2. Therefore it was concluded that the one-electron reduction of nimesulide proceeded with deprotonation.

Table 2. Theoretical and experimental frequencies and intensities for nimesulide dianion radical **3a**.

No	Theoretical data (B3LYP/6-311++G(2df,2dp))			Experimental data (DMSO-d$_6$[a])	
	$\nu_{theor.}$[b]	A[c]	Approximate description[d]	$\nu_{exp.}$	A[e]
1.	3079	1	ν_{PhA}(C-H)	-[f]	-[f]
2.	3074	5	ν_{PhA}(C-H)	-[f]	-[f]
3.	3063	3	ν_{PhB}(C-H)	-[f]	-[f]
4.	3055	4	ν_{PhA}(C-H)	-[f]	-[f]
5.	3054	24	ν_{PhB}(C-H)	-[f]	-[f]
6.	3046	33	ν_{PhA}(C-H)	-[f]	-[f]
7.	3034	16	ν_{PhB}(C-H)	-[f]	-[f]
8.	3028	4	ν_{PhB}(C-H)	-[f]	-[f]
9.	3020	7	ν^{as}(CH$_3$)	-[f]	-[f]
10.	3013	10	ν^{as}(CH$_3$)	-[f]	-[f]
11.	2929	11	ν^{s}(CH$_3$)	-[f]	-[f]
12.	1603	124	ν^{s}(CH$_3$)	1599	sh
13.	1592	35	ν_{PhB}(C=C)	1590	sh
14.	1578	50	ν_{PhB}(C=C)	1581	m
15.	1528	1	ν_{PhA}(C=C)	-[f]	-[f]
16.	1496	176	ν_{PhA}(C=C)	1500	sh
17.	1484	455	δ_{PhA}(C-H)	1492	s
18.	1467	1	δ_{PhB}(C-H)	1474	m
19.	1438	5	δ^{as}(CH$_3$)	-[f]	-[f]
20.	1436	2	δ^{as}(CH$_3$)	-[f]	-[f]
21.	1425	42	ν_{PhA}(C=C); δ_{PhA}(C-H)	-[f]	-[f]
22.	1348	395	ν(C-NO$_2$); δ_{PhA}(C-H)	1347	m
23.	1343	24	δ_{PhB}(C-H)	-[f]	-[f]
24.	1326	107	δ^{s}(CH$_3$)	1323	m
25.	1316	14	ν_{PhA}(C=C); δ_{PhA}(C-H)	1313	m
26.	1298	732	ν(C-NSO$_2$); δ_{PhA}(C-H)	1294	vs, sh
27.	1293	714	ν_{PhA}(C=C); δ_{PhA}(C-H)	1285	vs, sh
28.	1248	84	δ^{PhB}(C-H)	1264	m
29.	1236	520	ν(C-OC), δ_{PhA}(C-H)	1246	m
30.	1227	331	ν^{as}(NO$_2$), δ_{PhA}(CH)	1225	m
31.	1188	208	ν(CO-C), δ_{PhA}(C-H)	1191	w
32.	1183	34	δ_{PhB}(C-H)	1188	w
33.	1178	484	ν^{as}(SO$_2$), δ_{PhA}(C-H)	1186	w
34.	1175	5	δ_{PhB}(C-H)	-[f]	-[f]
35.	1137	165	δ_{PhA}(C-H)	-[f]	m
36.	1104	18	δ_{PhB}(C-H)	-[f]	m
37.	1085	390	ν^{s}(SO$_2$)	1109	-[f]
38.[g]	1058	12	ν^{s}(NO$_2$)	-[f]	-[f]
MAD[h]	-	-	-	8.6	-

[a] Measured after having decomposed the complex bands into components; [b] Infrared frequencies [cm[-1]] scaled by Eqn. (1); [c] Predicted intensities [km.mol^{-1}]; [d] Vibrational modes: ν, stretching; δ, in-plane bending; superscripts: s, symmetrical; as, asymmetrical; PhA, phenyl ring A; PhB - phenyl ring B; [e] Relative intensities: w, weak; m, moderate; s, strong; vs, very strong; sh, shoulder; [f] These bands were not detected in the IR spectrum; [g] Followed by 28 lower-frequency vibrations that could not be observed experimentally due to self-absorptions of DMSO-d$_6$ below 1100 cm^{-1}; [h] Mean Absolute Deviation between theoretically predicted and experimentally observed vibrational frequencies.
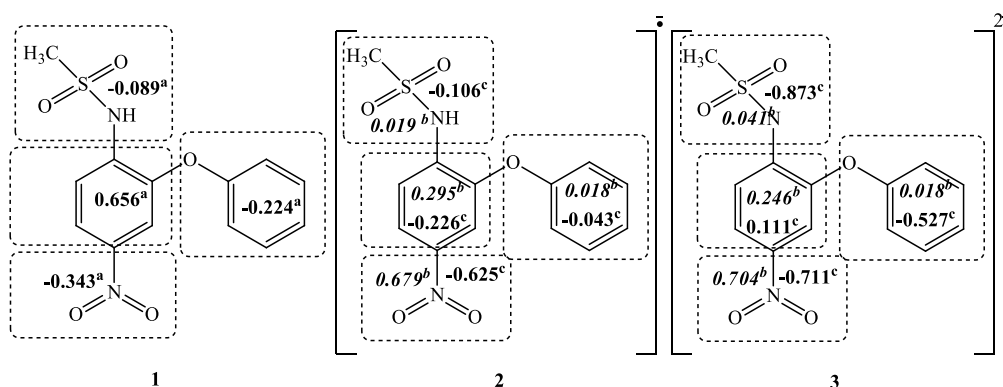
Fig. 3. Electron density distribution over fragments in nimesulide molecule **1** and its radical species **2** and **3**.
[a] NBO net electronic charges. [b] NBO electron spin density (in italics). [c] NBO electronic charge changes $\Delta q_i = q_i$ (radical) - q_i (molecule).

Structural analysis

The observed shifting of the bands of nitro and sulfonyl groups is in good agreement with the predicted changes in bond lengths. The S-O bonds are affected insignificantly by conversion in **2**, while conversion in **3** causes 0.025-0.032 Å lengthening of the S-O bonds and 0.008 Å shortening of the C-NSO$_2$ bond.

NBO electronic charges and spin density distribution over fragments of the studied species are shown in Figure 3. In the radical anion **2** 68% of the spin density and 63% from the anionic charge are concentrated into the nitro group (Figure 3). It can be concluded, that the structure of **2** is determined mainly by the localization of the single electron in the nitrophenyl fragment (96%). The results presented for dianion radical **3** are also indicative – 71% of the spin density is localized into the nitro group, whereas 87% of the anionic charge is concentrated into the sulfonamide fragment.

It can be summarized, that the topological characteristics of the structure determine sulfonyl group to be a weak competitor of the nitro group for the odd electron distribution and the opposite – the nitro group to be a weak competitor of the sulfonyl one for the anionic charge distribution.

CONCLUSION

The IR spectral changes arising in the course of electrochemical reduction of nimesulide, were studied in DMSO-d$_6$ solution with tetrabutyl-ammonium bromide as electrolyte salt. Based on comparison with theoretically predicted spectra of possible reduction products, *i.e.* (i) radical anion resulting from one-electron reduction and (ii) dianion radical resulting from one-electron reduction accompanied by deprotonation, it was concluded that in these conditions the electrochemical reduction of nimesulide leads to the generation of a dianion radical. A reliable interpretation of the spectral data was achieved by a combined experimental and theoretical IR approach. It was shown that conversion of nimesulide into dianion radical caused significant spectral and structural changes in the nitro and sulfonamide group and the phenyl ring connecting them. According to the NBO calculations, the major part of the spin density is localized into the nitro group of the dianion radical, whereas the most of the anionic charge is concentrated into the sulfonamide fragment.

Electronic Supplementary Data available here.

REFERENCES

1. H. Suleyman, E. Cadirci, A. Albayrak, Z. Halici, *Curr. Med. Chem.*, **15**, 278 (2008).
2. S. Agrawal, S. S. Pancholi, N. K. Jain, G. P. Agrawal, *Int. J. Pharm.*, **274**, 149 (2004).
3. G. F. Fabiola, V. Pattabhi, K. Nagarajan, *Bioorg. Med. Chem.*, **6**, 2337 (1998).
4. U. A. Boelsterli, *Int. J. Clin. Pract.*, **128**, 30 (2002).
5. U. A. Boelsterli, H. K. Ho, S. Zhou, K. Y. Leow, *Curr. Drug Metabol.*, **7**, 715 (2006).
6. R. Davis, R. N. Brogden, *Drugs*, **48**, 431 (1994).
7. A. Bernareggi, *Clin. Pharmacokinet.*, **35**, 247 (1998).
8. R. S. Borges, R.F. Matos, A.S. Carneiro, J.P. Oliveira, A.M.J.C. Neto, M.C. Monteiro, *J. Mol. Model.*, **21**, 166 (2015).
9. S. G. Kucukguzel, I. Kucukguzel, B. Oral, S. Sezen, S. Rollas, *Eur. J. Drug Metab. Pharmacokinet.*, **30**, 127 (2005).

10. F. W. P. Ribeiro, T. R. V. Soares, S. do N. Oliveira, L. C. Melo, J. E. Soares, H. Becker, D. De Souza, P. de Lima-Neto, A. N. Correia, *J. Anal. Chem.*, **69**, 62 (2014).

11. A. Alvarez-Lueje, P. Vasquez, L.J. Núñez-Vergara, J.A. Squella, *Electro-anal.*, **9**, 1209 (1997).

12. J. Squella, P. Gonzalez, S. Bollo, L. Núñez-Vergara, *Pharm Res.*, **16**, 161 (1999).

13. I. N. Juchnovski, Ch. Tsvetanov, I. Panayotov, *Monatsh. Chem.*, **100**, 1980 (1969).

14. I. N. Juchnovski, I. Binev, *Chem. Phys. Lett.*, **12**, 40 (1971).

15. I. Juchnovski, I. Binev, A. Fattah Nazir, J. Tsenov, *Commun. Depart. Chem. Bulg. Acad. Sci.*, **12**, 500 (1979).

16. I. N. Juhnovski, T. M. Kolev, I. G. Binev, *Dokl. Bulg. Acad. Sci.*, **30**, 1017(1977).

17. I. Juchnovski, T. Kolev, I. Rashkov, *Spectrosc. Lett.*, **18**, 171 (1985).

18. I. Juchnovski, T. Kolev, *Spectrosc. Lett.*, **19**, 529 (1986).

19. I. Juchnovski, T. Kolev, *Spectrosc. Lett.*, **19**, 1183 (1986).

20. I. Juchnovski, Ts. Kolev, *Spectrosc. Lett.*, **18**, 481 (1985).

21. I. N. Juchnovski, V. Ognyanova, G. N. Andreev, *Spectrosc. Lett.*, **27**, 1299 (1994).

22. S. Stoyanov, *J. Phys. Chem.*, **114**, 5149 (2010).

23. S. S. Stoyanov, D. Y. Yancheva, B. Stamboliyska, *Comp. Theor. Chem.*, **1046**, 57 (2014).

24. M.J. Frisch, G.W. Trucks, H.B. Schlegel, G.E. Scuseria, M.A. Robb, J.R. Cheeseman, V.G. Zakrzewski, J.A. Montgomery, R.E.S. Jr., J.C. Burant, S. Dapprich, J.M. Millam, A.D. Daniels, K.N. Kudin, M.C. Strain, O. Farkas, J. Tomasi, V. Barone, M. Cossi, R. Cammi, B. Mennucci, C. Pomelli, C. Adamo, S. Clifford, J. Ochterski, G.A. Petersson, P.Y. Ayala, Q. Cui, K. Morokuma, D.K. Malick, A.D. Rabuck, K. Raghavachari, J.B. Foresman, J. Cioslowski, J.V. Ortiz, A.G. Baboul, B.B. Stefanov, G. Liu, A. Liashenko, P. Piskorz, I. Komaromi, R. Gomperts, R.L. Martin, D.J. Fox, T. Keith, M.A. Al-Laham, C.Y. Peng, A. Nanayakkara, C. Gonzalez, M. Challacombe, P.M.W. Gill, B. Johnson, W. Chen, M.W. Wong, J.L. Andres, M. Head-Gordon, E.S. Replogle, J.A. Pople, Gaussian98, Gaussian, Inc., Pittsburgh PA, 1998.

25. P. J. Stephens, F. J. Devlin, C. F. Chabalowsky, M. J. Frisch, *J. Phys. Chem.*, **98**, 623 (1994).

26. J. Tomasi, B. Mennucci, E.J. Cances, *J. Mol. Struct. (THEOCHEM)*, **464**, 211 (1999).

27. J. Tomasi, M. Perisco, *Chem. Rev.*, **94**, 2027 (1994).

28. P. Bergese, E. Bontempi, I. Colombo, D. Gervasoni, L. Depero, *Compos Sci. Technol.,* **63**, 1197 (2003).

29. L. Dupont, B. Pirrotte, B. Masereel, J. Delarge, J.Geczy, Nimesulide, *J Acta Cryst C*, **51**, 507 (1995).

30. C. Michaux, C. Charlier, F. Julemont, B. Norberg, J.-M. Dogne, B. Pirotte, F. Durant, *Acta Cryst.*, **E57**, o1012 (2001).

31. P. Sanphui, B. Sarma, A. Nangia, *J. Pharm. Sci.*, **100**, 2287 (2011).

ИЧ СПЕКТРАЛНО ИЗСЛЕДВАНЕ НА ЕЛЕКТРОХИМИЧНАТА РЕДУКЦИЯ НА НИМЕЗУЛИД

С. Стоянов[*], Д. Янчева, А. Косатева

Лаборатория „Структурен органичен анализ“, Институт по органична химия с център по фитохимия, Българска академия на науките, ул. „Акад. Г. Бончев“, бл. 9, 1113 София, България

(Резюме)

Електрохимичната редукция на нестероидното противовъзпалително лекарство нимезулид, N-(4-нитро-2-феноксифенил)-метансулфонамид, беше проведена в разтвор на DMSO-d_6 и бяха проследени ИЧ спектралните промени, породени от превръщането. Спектралните изследвания показаха, че при тези условия електрохимичната редукция води до значително понижение на N-O и S-O валентните честоти, повишаване на C-NO_2 валентната честота и изчезване на δ(N-H). Въз основа на сравнението с теоретично предсказаните спектри на възможните редукционни продукти, наблюдаваните промени са отдадени на генерирането на дианион-радикал на нимезулида. Отместванията на ИЧ ивици свидетелстват, че в резултат на редукцията са настъпили значителни структурни промени в нитро-, сулфонамидната група и фенилното ядро, свързвано с тях. Според изчислените натурални заряди и спинова плътност, 71% от спиновата плътност е съсредоточена в нитрогрупата на дианион-радикала, докато 87% от анионния заряд е локализиран в сулфонамидния фрагмент.